Available online at www.sciencedirect.com
SCIENCE DIRECT
Polymer 46 (2005) 4544–4553
polymer
www.elsevier.com/locate/polymer

Thermal, morphological and rheological characterization of poly(acrylic acid-*g*-styrene) amphiphilic graft copolymers

J.L. de la Fuente[a,*], M. Wilhelm[b,c], H.W. Spiess[c], E.L. Madruga[d,1], M. Fernández-Garcia[d], M.L. Cerrada[d]

[a]*Instituto Nacional de Técnica Aeroespacial 'Esteban Terradas', I.N.T.A., Crta. de Ajalvir, Km 4, 28850 Torrejón de Ardoz, Madrid, Spain*
[b]*Max-Planck Research Group, TU-barmstadt, Germany*
[c]*Max-Planck Institut für Polymerforschung, Ackermannweg 10, 55128 Mainz, Germany*
[d]*Instituto de Ciencia y Tecnología de Polímeros (C.S.I.C.), Juan de la Cierva, 3, 28006 Madrid, Spain*

Received 7 February 2005; received in revised form 30 March 2005; accepted 30 March 2005
Available online 19 April 2005

Abstract

A family of amphiphilic poly(acrylic acid-*g*-styrene), P(AA-*g*-S), graft copolymers has been prepared by quantitative hydrolysis from poly(*tert*-butyl acrylate-*g*-styrene), P(*t*BA-*g*-S), precursors and evaluated by ^{1}H NMR and FTIR. The thermal characterization of these copolymers as a function of the number of grafted repeat units has been performed by thermogravimetric analysis, TGA, differential scanning calorimetry, DSC, and dynamic mechanical experiments. A higher thermal stability of the PAA main chain was observed by TGA as incompatible PS is grafted onto it. Small-angle X-ray scattering, SAXS, measurements have confirmed the existence of phase separation in the graft copolymers and the morphological behavior was analyzed. An increase on microdomains size is observed when the number of grafts diminishes. Moreover, the presence of polar functional groups in the backbone chain leads to the formation of hydrogen bonds giving rise to a substantial modification of the linear viscoelastic response compared with that exhibited by the unhydrolyzed precursory copolymers, as observed by analysis of melt rheological measurements.

Keywords: Poly(acrylic acid-*g*-styrene) amphiphilic graft copolymers; DSC; TGA

1. Introduction

Amphiphilic block copolymers are used now-a-days for a broad variety of applications [1], e.g. as polymeric surfactants, reactors for nanoparticles, thickening agents in paints, in cosmetics, for enhanced oil recovery, or as biomedical substances, etc. Block copolymers are of a considerable interest because of their ability to self-assemble in solution or bulk states. The widely extended range of potential industrial applications for amphiphilic block copolymer is a consequence of their particularly interesting tendency to self-associate in the aqueous medium [2], yielding microdomains with lowered polarity that can be incorporated and transport external hydrophobic molecules. On the other hand, a large number of their technological applications demand controlling the level of surface hydrophilicity or hydrophobicity. Depending on the application, it may be required that a given liquid wets the polymer surface (adhesion, printing, etc.) or on the opposite, it may involve a repellent polymer surface (waterproofing, oil or soil repellence, etc.). These current and potential future applications have provoked that polymeric solutions are gaining importance due to their unique and in a wide range adjustable physical and structural properties. Despite this, the solid-state properties of these materials have not received much attention compared with their solution behavior.

Linear block copolymers formed by hydrophilic blocks of polyacrylic acid (PAA) and hydrophobic chains of polystyrene (PS) have received a great interest in the last years [3]. Eisenberg and his group [3d–f] have studied the multiple morphologies and characteristics of 'crew-cut' micelle-like aggregates of PAA-*b*-PS diblock copolymers in

* Corresponding author. Tel.: +34 915 201 841; fax: +34 915 201 611.
E-mail address: fuentegj@inta.es (J.L. de la Fuente).
[1] Deceased December 2003.

0032-3861/$ - see front matter © 2005 Elsevier Ltd. All rights reserved.
doi:10.1016/j.polymer.2005.03.076

aqueous solution. On the other hand, Huang et al. [3g] have described the capacity of these copolymers to afford stable nanoscale particles. The formation of these nanostructured materials is due to the assembly of these amphiphilic diblock copolymers within an aqueous solution followed by crosslinking reactions selectively throughout core or shell domains. These copolymers have also been used as stabilizers in emulsion polymerization [3h]. In addition, the neutralization of PAA segments has permitted to prepare halato-telechelic copolymers [3a]. Recently, Tsitsilianis and Iliopoulos [4] have described the viscoelastic properties exhibited by a physical gel formed by charged PAA end-capped with PS sort blocks (PS-*b*-PANa-*b*-PS). The unique property shown by these gels is the possibility to control their viscoelasticity by changing the conformation of the elastic chains through the pH of the solution.

A good number of investigations about this system have been restricted to linear di- and tri-block copolymers, although in the last years, the preparation and the study of novel block copolymers with branched architecture (grafts, stars, dendrimers, hyperbranched, etc.) have successfully created materials possessing unusual behavior, in comparison with traditional linear block copolymers. This has also allowed opening up a whole new dimension in amphiphilic block copolymers research, namely the interplay between topology and morphology on solution and bulk properties [5]. Some examples in this area corresponds to the work of Müller and co-workers [6] about amphiphilic cylindrical brushes with PAA core and PS shell, or that of Francis et al. [7] where they describe the synthesis and characterization of novel PS(PAA)$_2$ miktoarm stars carrying one hydrophobic PS branch and two ionizable PAA arms. Concretely in the case of graft copolymers constituted by these two components, a PAA backbone and grafts of PS, only one article of Carrot et al. [8] describes, to our knowledge, the organization ability of these copolymers, to form micelles and at the same, these authors verified its ability to stabilize emulsions.

The topology or molecular architecture is a very important factor in the morphological behavior of block copolymers. While the morphology of linear, conformationally symmetric diblock copolymers relies entirely on the volume fraction of the respective blocks, the morphology of graft (and other branched block copolymers) also depends on an additional factor, the molecular asymmetry parameter. This asymmetry parameter contains a factor describing the conformational asymmetry between the two blocks and another factor describing the asymmetry inherent to the macromolecular architecture [9]. Hence, branched block copolymers are able to yield morphologies that cannot be developed by linear diblock copolymers at the same volume fraction. Benoit and Hadziioannou [10] proposed for graft copolymers a general theory to predict the scattering profiles in the homogeneous state and at the spinodal. They found that the scattering profiles of grafts copolymers as well as the spinodal curves were relatively insensitive to the total number of constituting units, approaching a limiting value at high number of units. Additionally, they found that the relevant values χN (χ being the Flory interaction parameter between both monomers and N the total number of monomeric units in the copolymer) for controlling phase behavior was that of the constituting unit rather than of the whole graft copolymer. A similar result was found by Balazs and co-workers when considered the behavior of order–disorder transition in graft copolymers [11].

The aim of this paper is study the structural and thermal–mechanical properties of a series of amphiphilic graft copolymers, poly(acrylic acid-*g*-styrene) P(AA-*g*-S) in their bulk state. The difference between the distinct graft copolymers is the number of graft incorporated onto the PAA backbone. These copolymers were prepared by total hydrolysis of poly(*tert*-butyl acrylate-*g*-styrene) graft precursory copolymers, P(*t*BA-*g*-S). The synthesis, thermal and viscoelastic properties, along with the morphological behavior of these graft precursors have been described in earlier papers [12]. These previous studies indicate phase separation and, thus, the existence of microdomains of both two components from above a certain degree of grafting.

2. Experimental

2.1. Graft copolymers

The methods used for the synthesis and characterization of graft copolymer precursors, P(*t*BA-*g*-S) were given in a previous paper [12a]. The preparation of the P(AA-*g*-S) was carried out as follows. P(*t*BA-*g*-S) copolymers were dissolved in an equal weight of dioxane (based on the mass of polymer added), and a three-fold excess of concentrated HCl was added (based on the moles of backbone ester groups). The flask was covered with a condenser, and the solution was heated to reflux. After 6 h, the solution was cooled, precipitated into hexane and then dried under vacuum to constant weight.

2.2. Characterization

The amphiphilic copolymer characterization was made by using KBr pellets in a FTIR Perkin–Elmer spectrum one and by proton nuclear magnetic resonance spectroscopy. ^{1}H NMR spectra were performed on Bruker AMX500 and DSX700 spectrometers. DMSO-d_6 (PAA-*g*-PS) or $CDCl_3$ (P*t*BA-*g*-PS) were used as solvents and using the deuterated proton signal as reference. Both techniques indicated a practically complete hydrolysis in all the samples.

The values of the apparent weight-average, number-average molecular weight, and number of grafts per chain along with copolymer composition of all the amphiphilic graft copolymers are listed in Table 1.

Table 1
Molecular characteristics of P(AA-*g*-S) amphiphilic graft copolymers and the homopolymers PAA and PS

Polymer	Calcd wt% PS[a]	wt% PS by ^{1}H NMR	$\bar{M}_n$[b]	$\bar{M}_w$[b]	N_{graft}
PAA	–	–	83,000	213,000	–
PAA-*g*-S1	32	29	113,000	301,000	7
PAA-*g*-S2	39	37	117,000	350,000	10
PAA-*g*-S3	50	47	128,000	409,000	15
PAA-*g*-S4	69	68	161,000	629,000	32
PS	–	–	13,000	13,650	–

[a] Calculated from the M_w values of grafted PS and graft copolymers.
[b] From SEC of the precursor graft copolymers, P(*t*BA-*g*-S), and recalculated after hydrolysis.

2.3. Specimen preparation

The samples of PAA, macromonomer PS, and the different P(AA-*g*-S) graft copolymers were prepared by compression molding, for dynamic mechanical and SAXS measurements, in a press between hot plates (disks with 8 mm of diameter and a thickness of approximately, 1 mm), at temperatures of 120 (PS) and 140 °C (PAA and PAA-*g*-PS), at a pressure of 2 MPa for 20 min, and subsequently, quenched to room temperature.

2.4. Glass transition temperatures

Glass transition temperatures, T_gs, were measured using a differential scanning calorimeter, Perkin–Elmer DSC/TA7DX, PC series with liquid nitrogen. The temperature scale was calibrated from the melting point of high purity chemicals (lauric and stearic acids and indium). Samples (~10 mg) were weighed and scanned at 10 °C/min from 30 to 150 °C under dry nitrogen (20 cm^3/min). Three consecutives scans were performed at 10 °C/min for each sample: heating/cooling/heating. The actual value for the T_g was estimated as the temperature at the midpoint of the line drawn between the temperature of intersection of the initial tangent with the tangent drawn through the point of inflection of the trace and the temperature of intersection of the tangent drawn through the point of inflection with the final tangent. The listed value is the average for several measurements conducted for each composition.

T_gs were also analyzed by dynamic mechanical properties measured with a Perkin–Elmer DMA7/TA7/DX analyzer working in a compression mode. The measuring system consisted of a 5 mm diameter parallel plate. Isochronal experiments were carried out with a heating rate of 2 °C/min (1 Hz frequency, 1% strain).

2.5. Thermal degradation

A Perkin–Elmer TGA-7 instrument was used for the thermogravimetric measurements. The instrument was calibrated both for temperature and weight by usual methods. Non-isothermal experiments were performed in the temperature range from 30 to 700 °C at heating rate of 10 °C/min. The average sample weight was 6 mg and the dry nitrogen flow rate was 20 cm^3/min.

2.6. Small-angle X-ray scattering

A Rigaku Rotaflex X-ray source with a wavelength of 0.154 nm Cu K_α was employed for small-angle X-ray scattering (SAXS) experiments. A three-pinhole collimator was used to generate a beam with a diameter of 0.1 mm. Scattering patterns were recorded on a two-dimensional Siemens X-100 area detector with a sample-to-detector distance of 145 cm. SAXS measurements were performed on compression-molded specimens and each profile was recorded at room temperature over a period of 2 h. The profiles are presented as a function of magnitude of scattering vector q, which is given by $q = (4\pi/\lambda)(\sin(\theta/2))$, where λ and θ are the wavelength of X-ray and the scattering angle, respectively. The scattered intensity is shown on a logarithmic scale in arbitrary units.

2.7. Rheological measurements

Rheological testing was performed with an advanced rheometric expansion system (ARES, Rheometrics Scientific) in the oscillatory mode with parallel-plate fixtures (8 mm) equipped with a 2KFRTN1-transducer. Dynamic frequency sweep experiments were conducted to measure the shear storage and loss moduli (G' and G'') as a function of angular frequency (ω) ranging from 0.1 to 100 rad/s at various temperatures (the highest temperature used did not exceed 180 °C). Master curves were constructed from the isothermal measurements in frequency sweeps using time–temperature superposition. Frequency sweeps required maintaining a constant gap between the plates (sample thickness) by compensating for tooling expansion/contraction with changes in the test. The strain applied to each specimen during testing was chosen to ensure that the obtained data were within the linear viscoelastic regime. All of the measurements were conducted under a nitrogen atmosphere in order to avoid oxidative degradation of the samples. Moreover, it was necessary to ensure that no significant degradation of the samples occurred at high temperatures. The initial frequency test was always

performed at 140 °C, and after testing at the highest temperatures for a particular specimen, the measurement at 140 °C was again repeated. In general, a very good agreement was observed between these two 140 °C measurements (initial and final one). Thus, no significant thermal degradation could be detected.

3. Results and discussion

The amphiphilic graft copolymers were obtained through acid-catalyzed hydrolysis in order to modify the ester groups of P*t*BA backbone to its acid form. FTIR and ^{1}H NMR determined the degree of hydrolysis of the resulting polymers. In all cases, conversions of *tert*-butyl ester groups into carboxylic acids were higher than 90%. Fig. 1(a) shows the FTIR spectra of a graft copolymer sample recorded before (P*t*BA-*g*-S4) and after (PAA-*g*-S4) hydrolysis with HCl. Hydrolysis is clearly responsible for the occurrence of a broad absorption between 3400 and 2400 cm^{-1}, which is characteristic of the OH groups, and the doublet band at ~1400 cm^{-1} corresponding to the stretching vibration of $-CH_3$ groups totally disappears after hydrolysis. Fig. 1(b) shows the disappearance of the resonance at 1.39 ppm, which is characteristic of the protons of the *tert*-butyl groups. The remaining resonance at ~1.4 ppm, still present after hydrolysis, is assigned to the β-methylene protons of the styrene segments that generally lead to a multiplet centered at 1.5 ppm.

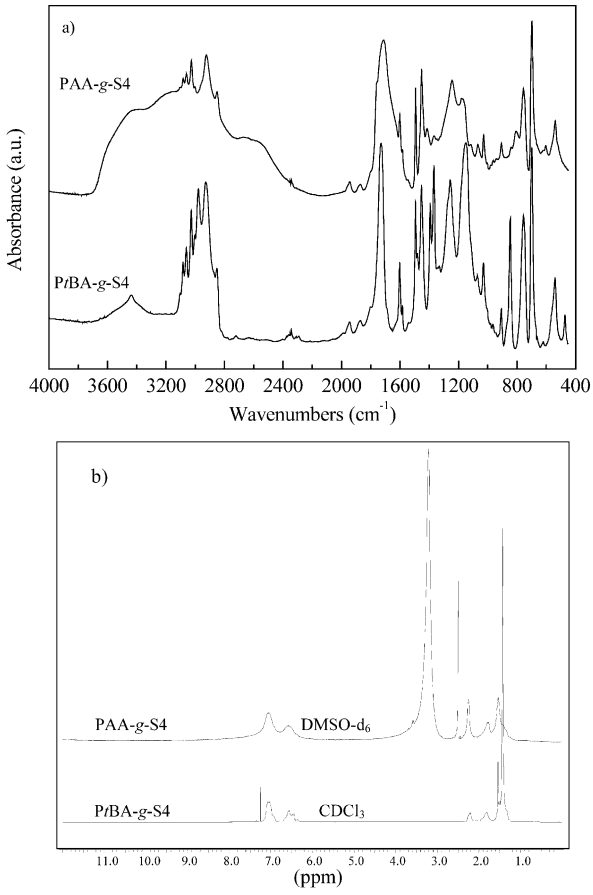

Fig. 1. (a) FTIR spectra and (b) ^{1}H NMR spectra of a graft copolymer before (P*t*BA-*g*-S4) and after (PAA-*g*-S4) hydrolysis with HCl.

3.1. Thermal characterization

The TGA and the related derivative, DTG, curves of the different copolymers as well as PAA and PS macromonomer under nitrogen at 10 °C/min are shown in Fig. 2(a) and (b), respectively. It is well established [13] that the decomposition of PAA is related to three main processes; dehydration, decarboxylation and chain scission. The dehydration could occur by intra or intermolecular reaction of carboxyl groups. Temperatures above 200 °C are required, so that intermolecular reactions occur. Probably these reactions between COOH that are left isolated after random intramolecular dehydration has taken place at slight lower temperatures. This would involve adjacent monomer units. The intramolecular reaction leads to the formation of six-membered glutaric anhydride type rings. The decarboxylation to give carbon dioxide becomes increasingly important above 250 °C and both water and carbon dioxide continue to be evolved on heating up to 500 °C. Chain scission occurs above 350 °C, where the formation of significant amounts of cold ring fraction consisting of dimer, trimer, etc. are possible due to release of fragments with short sequences of acrylic acid units, previously isolated between anhydride rings. Finally, the chain scission occurs adjacent to the anhydride rings, followed by further

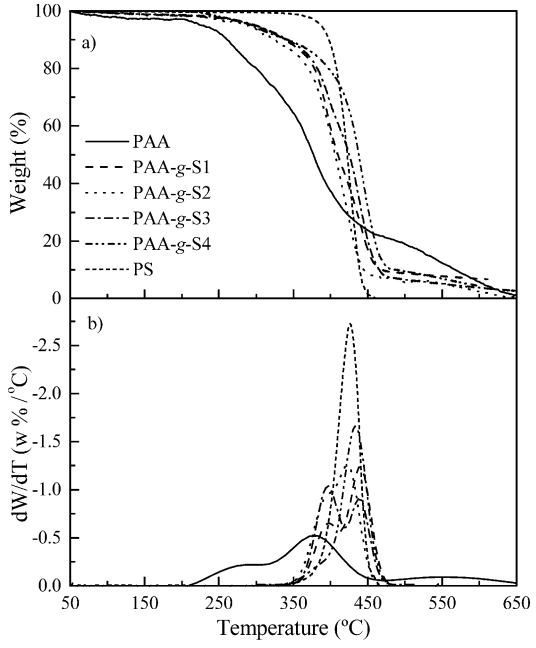

Fig. 2. Themogravimetric curves and their derivatives for PAA, PS macromonomer and P(AA-*g*-S) graft copolymers under a nitrogen atmosphere, at a heating rate of 10 °C/min.

reaction of the generated macroradicals. On the other hand, the decomposition of polystyrene macromonomer is detected in a single sharp step around T_{max} at 426.0 °C.

The degradation in the P(AA-*g*-S) graft copolymers takes place through two clear stages: the first one is mainly associated with dehydratation and decarboxylation reaction of the backbone similar to PAA degradation. The second stage is attributed to the degradation reaction by either the chain scission of branches or backbone. The temperatures of 5%, 50% mass loss, $T_{5\%}$, $T_{50\%}$ and the two maximum rate temperatures of weight loss, T_{max}, corresponding to the first and second stages as well as the area percentage of the maxima are collected in Table 2. The 5% weight loss temperature has been taken for simplicity as an index to assess the thermal stability. The variation of $T_{5\%}$ as graft number increases is very slight, however, the $T_{50\%}$ notably increases with that content, which indicates the stability enhances due to polystyrene being incorporated in the backbone. The two maximum rate temperatures of weight loss between copolymers remain largely unchanged, but there is a significant shift to higher temperatures compared to PAA and PS macromonomer. Therefore, when polystyrene is grafted, a higher thermal stability of the main chain is achieved. The DTG curves have been deconvoluted using modified Gaussian curves and assuming a linear background over the temperature range of the fit. The area percentage of the first peak decreases while the second peak area increases as the PS content is raised. The related integrals are in agreement with the related PS content in the copolymer.

DSC, dynamic mechanical measurements, SAXS and, more recently, solid-state NMR are some of the techniques, which allow to determine the existence of phase segregation of amphiphilic copolymer systems [14]. Amorphous block and graft copolymers with a microphase separated structure present two different T_gs dependent mainly on the molecular weights of the corresponding blocks and the copolymer composition. T_gs values determined by DSC are collected in Table 2 for the copolymers under study. A single glass transition temperature is detected in all of the DSC thermograms except in PAA-*g*-S4 copolymer that contains the highest number of branches and exhibits two glass transitions. The main transition assigned to the PAA backbone is significantly moved toward higher temperatures in the graft copolymers compared to the PAA homopolymer, as expected. This shift is probably due to the introduction of rigid PS as a side segment in the PAA backbone that imposes a hindrance to this cooperative motion. A second transition around 132 °C is observed just for PAA-*g*-S4 copolymer and is correlated to long-range segmental motions within PS grafts. This transition is also shifted to higher temperature than the T_g found in the macromonomer (~97 °C). The fact that a T_g is higher in the copolymer than in either the pure backbone or pure graft is rather unusual, although there are some examples in the literature. Yao et al. [15] found in poly(vinyl alcohol)-*g*-poly(methyl methacrylate) (PVA-*g*-PMMA) graft copolymers that the main chains also increased the T_g of the side methacrylic chains whereas the data reported by Xu et al. [16] for poly(styrene)-*g*-poly(ethylene oxide) (PS-*g*-PEO) graft copolymers showed that the T_g of the PS was moved up to 118 °C. As a result, the main chain and side chain reduce the mobility each other in these graft copolymers. In the PAA-*g*-S copolymers analyzed, this behavior might be associated with the existence in these copolymers of hydrogen bonds between carboxylic acid groups that lead to an increase of backbone interactions. Such interactions reduce the mobility of the whole polymeric material and, therefore, the occurrence of generalized motions within PS grafts shifts to higher temperatures. The importance of these hydrogen bonds in the rheological behavior will be discussed in a next section.

Dynamical mechanical isochronal temperature sweep measurements (at 1 Hz) of the samples also probe the microphase separation in the copolymers under study, as observed clearly in Fig. 3. This figure shows temperature scans of loss tangent, tan δ (E''/E'), for different graft copolymers and the corresponding linear homopolymers. PAA shows a broad peak centered at about 98 °C assigned to its T_g, while for PS macromonomer, it is observed that after this cooperative relaxation occurs the tan δ values start to considerably increase due to its low molecular weight. The PS graft M_n is lower than average molecular weight of chain entanglement and, therefore, the flow immediately starts to occur. All graft copolymers exhibit a well-defined maximum related to the cooperative movements of the PAA backbone, as shown in this figure. The peak maximum is shifted to higher temperatures as the graft content increases

Table 2
Glass transition temperature and temperature of 5 and 50% mass loss, $T_{5\%}$, $T_{50\%}$, temperature of the first and second maximum, T_{max}, and area percentages of the maximums corresponding to each amphiphilic graft copolymer and homopolymers

Polymer	T_g[a] (°C)	$T_{5\%}$ (°C)	$T_{50\%}$ (°C)	T_{max1} (°C)	$Area_{max1}$ (%)	T_{max2} (°C)	$Area_{max2}$ (%)
PAA	79.5	227.5	377.3	282.7	27.2	378.3	72.8
PAA-*g*-S1	91.8	288.5	406.3	396.3	58.4	439.4	41.6
PAA-*g*-S2	95.6	292.2	410.0	393.6	52.3	425.9	47.7
PAA-*g*-S3	96.5	290.4	425.2	396.6	38.5	440.3	61.5
PAA-*g*-S4	100.5, 131.6	297.7	437.9	397.3	20.7	434.0	79.3
PS	98.4	386.9	422.7	–	–	426.0	–

[a] Determined by DSC.

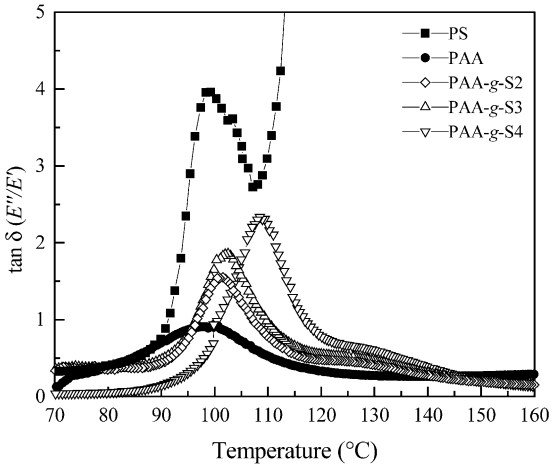

Fig. 3. Plots of tan δ versus temperature for several of P(AA-*g*-S) copolymer samples and the corresponding homopolymers, PAA and PS using DMA at 1 Hz excitation frequency.

due to the movement hindrance introduced by these grafts. Moreover, a second relaxation related to the glass transition of PS grafted chains is observed in copolymers with a number of grafts of 10 or higher using DMA. It has to be noted that this process could only be detected by DSC for the PAA-*g*-S4 sample. Therefore, the DMA technique seems to be more sensitive to identify the existence of phase separation between the two components within these graft copolymers [12b]. This relaxation is detected as a shoulder overlapping the relaxation related to T_g of the PAA backbone. Its intensity clearly increases and its maximum is shifted to higher temperatures as the number of PS graft content is raised, because of the larger mobility restrictions existing in the copolymer. The different T_g values are collected in Table 3, correlating well with those already found by calorimetric measurements.

3.2. SAXS analysis

The bulk structural organization of these graft copolymer systems was studied by 1D and 2D SAXS measurements. Fig. 4 displays the SAXS profiles plotted against the scattering vector, q, for the different amphiphilic graft copolymers at room temperature. The incident X-ray beam

Table 3
Morphological and rheological properties of the P(AA-*g*-S) graft copolymers and PAA and PS homopolymer samples (reference temperature 120 °C)

Polymer	T_g[a] (°C)	C_1	C_2 (K)	D^* (nm)[b]
PAA	98	7.5	79.4	–
PAA-*g*-S1	100	11.4	79.5	–
PAA-*g*-S2	101, 126	8.9	80.2	31.4
PAA-*g*-S3	102, 127	8.6	74.2	32.9
PAA-*g*-S4	109, 129	10.1	74.6	21.1
PS	100	8.3	83.1	–

[a] Estimated by dynamic mechanical measurements (tan δ).
[b] Primary SAXS reflection, $D^* = 2\pi/q^*$.

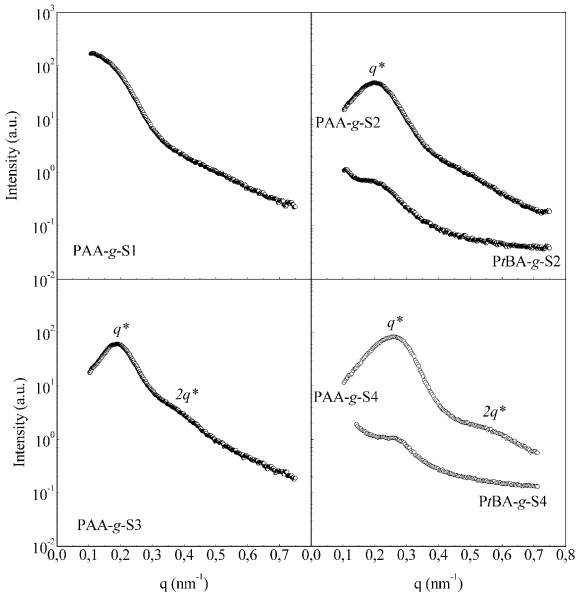

Fig. 4. Small-angle X-ray scattering intensities as a function of the scattering vector, q, for P(AA-*g*-S) graft copolymer samples. Several non-hydrolyzed P(*t*BA-*g*-S) 'parent' copolymers are also plotted for comparison.

was normal to the sample surface (through-view scattering). Circular patterns of scattered intensities were obtained from the two-dimensional detector, implying that no preferential orientation of microdomains was developed globally. One of the specific features of these SAXS plots is that the sample with the lowest PS grafted content, PAA-*g*-S1, does not exhibit a Bragg peak. The absence of reflections agrees with the results obtained by DSC and dynamic mechanical analysis, just described, and with the SAXS data obtained in its corresponding unhydrolyzed precursory copolymer [12c]. However, the copolymers with higher PS content show a strong primary scattering peak followed by a weak shoulder that can be ascribed to a second order peak. This second order peak is better defined in PAA-*g*-S4 confirming that this copolymer exhibits the strongest phase segregation. The position of Bragg peaks seems to move to higher q value with increasing fraction of PS in the copolymer. However, no long-range order correlations are exhibited by these samples. The relative peak positions at q_n/q^* ratio of 1 and 2 could suggest the presence of an approximately lamellar morphology for the three copolymers with the highest PS contents. This lamellar organization is in agreement with the volume fraction of the specimens if behaviour similar to a linear diblock copolymer is assumed. It is important to note that for graft architectures (and other branched polymer material), each of the established morphologies, i.e. spheres, cylinders, lamellae, etc. is observed at a higher PS graft volume fraction than would be expected in a simple diblock copolymer [9]. Although a lamellar structure is certainly a more likely scenario for these P(AA-*g*-S) samples the peaks are too broad to allow a conclusive assignment. Bendejacq et al. [3b] have analyzed

some solvent-cast films of linear PAA-*b*-PS diblock copolymer and found similar results. The authors of [3b] observed lamellar or hexagonally packed cylindrical morphologies for copolymers in the middle composition range (in some samples with little long-range order). Some of those diblock copolymers with greater compositional asymmetry exhibited even spherical microdomains without lattice order.

The absence of less prominent peaks at higher orders for asymmetric PAA-*b*-PS diblock copolymers is well-established in the literature for other asymmetric block copolymers, such as graft copolymers [17,18]. In general, these materials develop the domain shape (spheres, cylinders, or lamellae) predicted by theory, though spherical and cylindrical morphologies have reduced long-range lattice order compared to those found in diblocks and other simpler molecular architectures. However, some long-range order is, at least, present in the lamellar morphologies, due to the space filling requirements of the lamellar domains.

The morphology depends additionally strongly on the sample preparation method and, unfortunately, the annealing of PAA at elevated temperature, well above the PS glass transition temperature to push organization toward equilibrium, is precluded due to its susceptibility to degradation and crosslinking.

Values of the interdomain spacing, D, were calculated from the position of the first-order peak q^* as $D=2\pi/q^*$ and are listed in Table 3. An increase of graft density in the copolymers leads to a reduction of the microdomains size. This feature might be associated either with the shortening of backbone block between grafts as the graft density raises or with a disentanglement of the backbone, sketched in the Fig. 5, with increasing number of grafts. This result is in agreement with theoretical predictions of Benoit and Hadziioannou [10] for homogeneous grafted copolymers and with experimental data obtained either by Biver et al. [19] in amphiphilic grafted copolymers based on a hydrophilic poly(vinyl alcohol) backbone and hydrophobic palmitic side chains, or by Gido and Hadjichristidis in copolymers with chain of PS grafted on polyisoprene backbone [17]. In fact, even in homopolymers, incompatibility between polymer backbone and side groups can lead to locally lamellar structures [20].

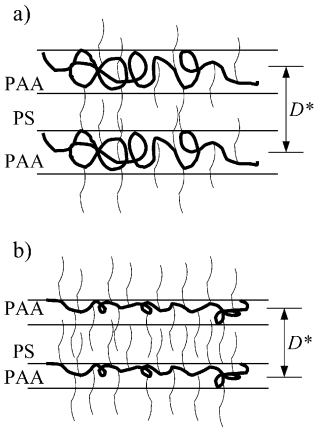

Fig. 5. Model representation of the organized domains in P(AA-*g*-S) copolymers with (a) low and (b) high number of grafts.

Fig. 4 also shows the SAXS curves at room temperature for several non-hydrolyzed P(*t*BA-*g*-S) copolymers. There is evidences of a stronger microphase separation in P(AA-*g*-S) copolymers than in their precursors possibly due to the larger interaction parameter χ between PS and PAA blocks than between PS and P*t*BA. Therefore, a well-defined maximum appears in the SAXS data accompanied by a significant increase in the scattering intensity for the P(AA-*g*-S) copolymers, probably related with the lower electron density contrast between the constitutive blocks within the former P(*t*BA-*g*-S) copolymers compared with that existing in the amphiphilic P(AA-*g*-S) copolymers. Another remarkable feature evident from a comparison of both series is that the primary reflection is located at similar scattering vector q^*. This fact indicates that after hydrolysis of the P*t*BA segments, the possible reorganization due to the possible association of the polar acid groups must be severely limited. Therefore, the high molecular weight and multiple junction points of these materials reduce the molecular mobility necessary for promoting this process.

3.3. Rheological behavior

The occurrence of a phase-separated microstructure strongly affects the linear viscoelastic response of block copolymer systems, especially at long time/low frequency. In addition, the presence of functional groups might give rise to macromolecular structures formed by non-covalent associations (e.g. dipolar interactions or H-bonding) due to the affinity for one to another. These macromolecular structures caused by the assembly of repeating units on different chains (interpolymer) or on separate regions of the same chain (intrapolymer) have been demonstrated to be a important factor in the thermo–mechanical properties of these materials [21]. Therefore, the influence of the microstructure and the molecular architecture on the rheological response of these graft copolymers is analyzed and compared with that exhibited by the corresponding unhydrolyzed precursors.

For the rheological characterization master curves were constructed applying time–temperature superposition, TTS, to the isothermal dynamic frequency sweep data in the temperature range from 70 to 180 °C, Fig. 6. Excellent superposition of both shear storage modulus, G', and shear loss modulus, G'', was observed in both linear homopolymers, PAA and PS, and graft copolymers. The horizontal shift factors, a_T, used to superimpose the curves and validate TTS fitted the WLF equation [22] and the parameters C_1 and C_2 calculated are listed in Table 3. The application of TTS to thermorheological complex liquids such as block copolymers deserves some comments, since there are two

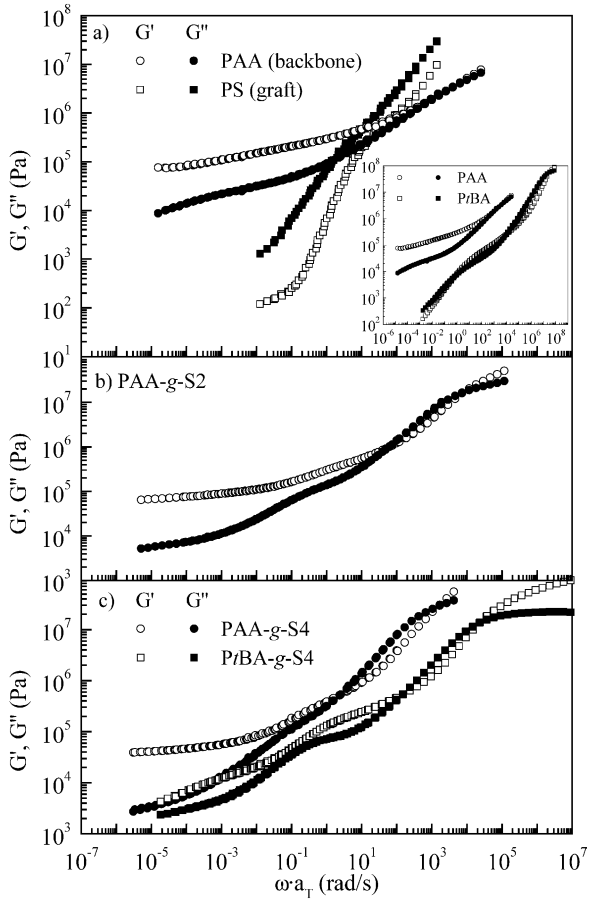

Fig. 6. Dynamic moduli-frequency master curves, storage (G', open symbols) and loss (G'', solid symbols), for homopolymers (PAA and PS) and several copolymers (P*t*BA-*g*-S4 is also included). Plot inset (a) shows master curves for P*t*BA homopolymer for comparison. Reference temperature is 120 °C.

temperature-dependent monomeric friction coefficients in the system (corresponding to the PS and PAA rich microdomains), the investigated systems do not have a linear topology and the morphology is itself temperature dependent. However, although there are two monomeric friction coefficients in these copolymers, the relaxation time scales of the PAA and PS domains are very similar (due to small difference in both T_gs). This fact may explain why applying TTS still leads to attain well-defined master curves.

To investigate the possible role of segmental interactions between the constituent blocks, the different viscoelastic properties exhibited in both 'parent' components, the PAA backbone and the side chains of PS should be known. In Fig. 6(a), the two homopolymers (PAA and PS) are shown at reference temperature of 120 °C. The curves for PAA only show the transition and the rubbery plateau regions, so that PAA does not flow in the experimental range analyzed and, therefore, the terminal region is not reached. The main striking feature of the rheological behavior of this homopolymer is the very broad rubbery plateau. The response of this structure in this regime is reflected in the dominant elasticity ($G' > G''$), indicating extensive associations. The viscoelastic behavior of PAA is totally different from that shown by its unhydrolyzed precursor, P*t*BA, as it can be observed in the plot insert in Fig. 6(a), where both master curves are included for comparison (the reference temperature is also 120 °C). The curve for the P*t*BA shows the usual transition, rubbery plateau and terminal regions typical for entanglement linear homopolymer. This plot clearly demonstrates that when a polymeric chain is chemically modified with acid groups as in the present study, promoting the formation H-bonds, its viscoelastic properties significantly change, e.g. factor 10^3 for G' at low frequencies. The new functional groups provoke a stable elastic network that dominates the broad viscoelastic spectrum. Dong and co-workers [23] described the coexistence of various types of hydrogen forms in PAA homopolymers, and the fact that these different structures of hydrogen bonds persisted even when the temperature rose well above the T_g. In Fig. 7, the four possible forms of carboxylic groups in the condensed phases are represented. On the other hand, the viscoelastic behavior for the PS macromonomer is typical of polymer melts of low molecular weight below the average molecular

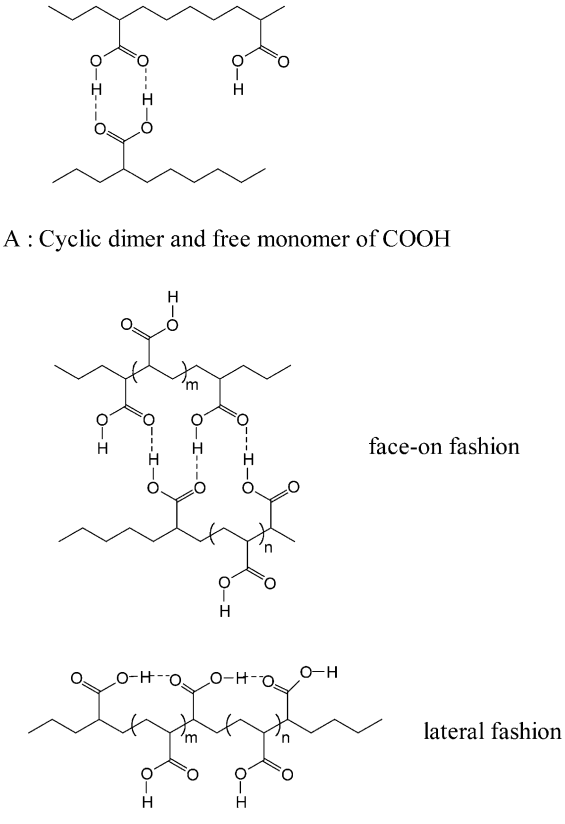

A : Cyclic dimer and free monomer of COOH

B: Inner and terminal COOH in linear oligomeric forms

Fig. 7. Four possible forms of carboxylic acid groups in the condensed phases: cyclic dimer, free monomer, and inner and terminal COOH groups in oligomeric forms [28].

weight between entanglement (which is about 17 kg/mol [22]) and the viscous component dominates its response to the deformation field.

The lower plots, Fig. 6(b) and (c), depict the master curves for the same two magnitudes, G' and G'', in the graft copolymers with very different graft density, samples PAA-*g*-S2 and PAA-*g*-S4, at a reference temperature of 120 °C. The entire range of viscoelastic behavior is not observed, since the terminal region was not accessed for the samples. Small differences can be observed comparing these two curves with the linear viscoelastic spectra of the PAA homopolymer. At high frequencies, both copolymers exhibit a slight shift of the cross-over frequencies from segmental to Rouse-like dynamics in comparison with PAA. This is attributed to the fraction of non-entangled glassy polystyrene that slows down the overall dynamics of the graft copolymer.

However, at low frequencies (Fig. 6(a–c)) no significant changes are observed for the PAA copolymers regime in comparison with PAA homopolymer. The dynamic moduli frequency curves of the graft copolymers show a weak inflexion in the plateau region and, therefore, this broad rubbery plateau is characterized by the existence of two regimes. A primary apparent plateau at higher frequencies occurs due to the relaxation of the grafts. It is better defined as the number of PS grafts on the main chain increases, and is particularly obvious in the shape of G'' curves. After the graft relaxation takes place, the rheological response is dominated by additional relaxation of the backbone before that microstructure governs the viscoelastic behavior. This response has been described in the P*t*BA-*g*-S precursor copolymers, [12c] where, at low frequencies, the onset of a secondary apparent plateau appears when the grafts are completely relaxed (Fig. 6(c)). This observation is attributed to the relaxation of the backbone (i.e. all the segments of the graft copolymer between two graft points). However, the strong association between the acid groups within the domains results in a network with a great stability, even at high temperatures above 120 °C that affects the viscoelastic properties in the graft copolymer under study. Since, in the PAA homopolymer the presence of distinct hydrogen-bond structures has been reported [23], it seems logical to consider the possibility that these copolymers might lead to the formation of this type of secondary interactions. In addition, spectroscopic evidences of such structures of PAA polymeric chains have been described in statistical copolymers, for instance PS-PAA [24,25] and poly(ethylene-*co*-methacrylic acid) [26,27]. Therefore, it is reasonable to assume that at low frequencies, PS chains affect only slightly the viscoelastic properties of the backbone. PS grafts act as viscous fluid within the hydrophilic matrix of PAA and only a slight reduction in the G' values in the plateau zone for graft copolymers with respect to that found in PAA homopolymer is observed.

The loss tangent is independent of the absolute module and, therefore, provides the most reliable and generally

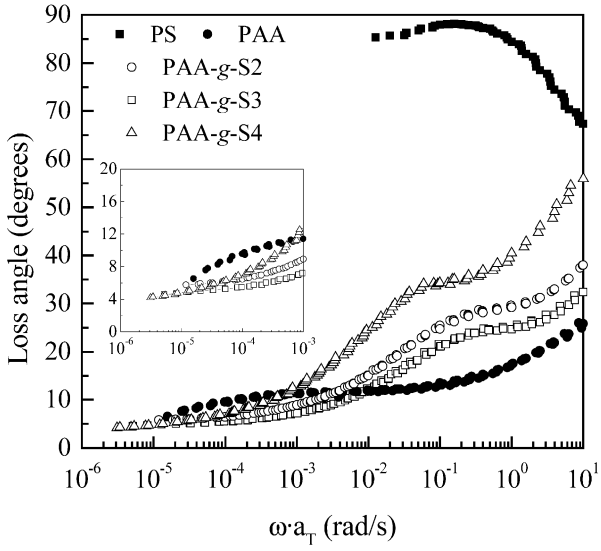

Fig. 8. Plots of loss angle as a function of the frequency for several P(AA-*g*-S) copolymers. PAA and PS homopolymers data are also plotted for reference.

valid rheological method to determine the presence of long-range connectivity in polymeric material, resulting from chemical or physical interactions (such as crystallinity, hydrogen bonds, phase-separated domains, etc.). Fig. 8 shows the variation of loss angle δ as a function of frequency and significant differences for PAA, PS macromonomer, and the amphiphilic copolymers are observed. For PS, at low values of frequency, δ is nearly 90°, meaning that the sample response is almost entirely viscous. The behavior for PAA homopolymer markedly differs from that exhibited by PS. This might be attributed to the formation of hydrogen bonds in PAA, previously mentioned, showing a behavior predominantly elastic. Also, a decrease of δ is observed for the distinct copolymer systems indicating that they become more elastic as the number of grafts increases. Moreover, the differences in the area under the curves follow the degree of grafting, as seen in this figure. These experimental observations can be interpreted by considering that the PS chains alter the hydrogen bonds between carboxylic acid groups (producing an increase of intermolecular interactions in certain regions of the backbone). It is also important to note, however, that the different degrees of both order and overall disorder developed in the distinct copolymers also can affect the elasticity in the low frequency regime.

In conclusion, a family of amphiphilic poly(acrylic acid-*g*-styrene), P(AA-*g*-S), graft copolymers is prepared by hydrolysis from poly(*tert*-butyl acrylate-*g*-styrene), P(*t*BA-*g*-S), precursors. The degree of hydrolysis is evaluated by ^{1}H NMR and FTIR. Dynamic mechanical analysis is more sensitive than DSC measurements to detect the phase segregation in these copolymers. The existence of domains steaming from both components is confirmed by SAXS experiments that point out that the phases are probably arranged in a less defined or less extended lamellar

morphology. On the other hand, the rheological analysis shows the importance of H-bond interactions in the response of these amphiphilic graft copolymers compared to that found in polymers without associating groups. A power law dependence of dynamic moduli over a range of two decades is observed in the PAA-*g*-S copolymer series. G' curves for the different copolymers progressively reach a practically purely elastic dependence, totally different from that exhibited for unhydrolyzed copolymers on the same range of frequencies ($G' \sim G'' \sim \omega^n$ with $n \approx 0.4$). The second characteristic deals with the increase on the G' values in the rubbery plateau in comparison with those found in the precursors copolymers.

Acknowledgements

This research has been supported by the Comisión Interministerial de Ciencia y Tecnología, project MAT2002-00250, and the EU-project CAPS (Complex Architecture in Diblock Copolymer Based Polymer Systems), FMRX-CT97-0112 (DG 12-DLCL).

References

[1] (a) Kennedy JP. Pure Appl Chem 1994;A31(11):1771.
(b) Forster S, Antonietti M. Adv Mater 1998;10(3):195.
(c) Fischer A, Brembilla A, Lochon P. Polymer 2001;42(4):1441.
(d) Ringsdorf H, Schlarb B, Wenzmer J. Angew Chem Int Ed Engl 1988;27:113.
(e) Chen J, Jiang M, Zhang Y, Zhou H. Macromolecules 1999;32:4861.
(f) Zhang Y, Li M, Fang Q, Zhang YX, Jiang M, Wu C. Macromolecules 1998;31:2527.
(g) Chassenieux C, Nicolai T, Durand D. Macromolecules 1997;30:4952.
(h) Xie X, Hogen-Esch TE. Macromolecules 1996;29:1734.
(i) Hillmyer MA, Bates FS. Macromolecules 1996;29:6994.
(j) Alexandridis P, Lindman B, editors. Amphiphilic block copolymers. Self-assembly and applications. Amsterdam: Elsevier, Science BV; 2000.
[2] (a) Dubin PB, editor. Microdomains in polymer solutions. New York: Plenum Press; 1986.
(b) McCormick CL, Hoyle CE, Clark MD. Polymer 1992;33:243.
(c) Cochin D, Zana R, Candau F. Polym Int 1993;30(4):491.
(d) Anton P, Köberle P, Laschewsky A. Makromol Chem 1993;194:1.
(e) Zhao CL, Winnick MA, Riess G, Croucher MD. Langmuir 1990;6(2):514.
[3] (a) Hautekeer J-P, Varshney SK, Fayt R, Jacobs C, Jérôme R, Teyssié Ph. Macromolecules 1990;23:3893.
(b) Bendejacq D, Ponsinet V, Joanicot M, Loo Y-L, Register RA. Macromolecules 2002;35:6645.
(c) Hawker CJ. J Am Chem Soc 1994;116:11185.
(d) Zhang L, Eisenberg A. Science 1995;268:1728.
(e) Zhang L, Eisenberg A. J Am Chem Soc 1996;118:3168.
(f) Yu Y, Eisenberg A. J Am Chem Soc 1997;119:8383.
(g) Huang H, Remsen EE, Wooley KL. Chem Commun 1998;1415.
(h) Burguière C, Pascual S, Bui C, Vairon JP, Charleux B, Davis KA, et al. Macromolecules 2001;34:4439.
[4] Tsitsilianis C, Iliopoulos I. Macromolecules 2002;35:3662.
[5] Pakula T. Macromol Symp 2004;214:307.
[6] Cheng G, Böker A, Zhang M, Krausch G, Müller AHE. Macromolecules 2001;34:6883.
[7] Francis R, Lepoittevin B, Taton D, Gnanou Y. Macromolecules 2002;35:9001.
[8] Carrot G, Hilborn J, Knauss DM. Polymer 1997;38:6401.
[9] Milner ST. Macromolecules 1994;27:2333.
[10] Benoit H, Hadziioannou G. Macromolecules 1988;21:1449.
[11] Shinozaki A, Jasnow D, Balazs AC. Macromolecules 1994;27:2496.
[12] (a) Fernández-García M, de la Fuente JL, Cerrada ML, Madruga EL. Polymer 2002;43:3173.
(b) Cerrada ML, de la Fuente JL, Madruga EL, Fernández-García M. Polymer 2002;43:2803.
(c) De la Fuente JL, Fernández-García M, Cerrada ML, Madruga EL, Spiess HW, Wilhelm M. In preparation.
[13] McNeill IC, Sadeghi SMT. Polym Degrad Stab 1990;29:233.
[14] Domján A, Erdödi G, Wilhelm M, Neidhöfer M, Landfester K, Iván B, et al. Macromolecules 2003;36:9107.
[15] Yao YM, Liu LZ, Li H, Fang TR, Zhou EL. Polymer 1994;35:3122.
[16] Jun-Ting X, Jian J. Polymer 2003;44:6379.
[17] Beyer FL, Gido SP, Buschl C, Iatrou H, Uhrig D, Mays JW, et al. Macromolecules 2000;33:2039.
[18] Xenidou M, Beyer FL, Hadjichristidis N, Gido SP, Tan NB. Macromolecules 1998;31:7659.
[19] Biver C, de Crevoisier G, Girault S, Mourran A, Pirri R, Razet JC, et al. Macromolecules 2002;35:2552.
[20] Wind M, Graf R, Renker S, Spiess HW, Steffen W. J Chem Phys 2005;122:1.
[21] Fredrickson GH, Bates FS. Ann Rev Mater Sci 1996;26:501.
[22] Ferry JD. Viscoelastic properties of polymer. 3rd ed. New York: Wiley; 1980.
[23] Dong J, Ozaki Y, Nakashima K. Macromolecules 1997;30:1111.
[24] Nyquist RA, Platt AE, Priddy DB. Appl Spectrosc 1982;36:417.
[25] Wang LF, Pearce EM, Kwei TK. J Polym Sci, Part C 1990;28:317.
[26] Lee JY, Painter PC, Coleman MM. Macromolecules 1988;21:346.
[27] Czarnecki MA, Liu Y, Ozaki Y, Suzuki M, Iwahashi M. Appl Spectrosc 1993;47:2162.
[28] Strictly speaking, the term oligomer here for carboxylic acid groups is different from the concept of oligomer in polymer science. The latter is built up by the repetition of small, simple chemical units through covalent bonds, whereas the former is interconnected through hydrogen bonds.